

Bacteriophage S6 requires bacterial cellulose for *Erwinia amylovora* infection

Leandra E. Knecht,^{1,2} Nadine Heinrich,^{2†}
Yannick Born,^{1‡} Katja Felder,^{2#} Cosima Pelludat^{1,3} ,³
Martin J. Loessner^{1,2}  and Lars Fieseler^{1*} 

¹Food Microbiology Research Group, Institute of Food and Beverage Innovation, Zurich University of Applied Sciences (ZHAW), Wädenswil, Switzerland.

²Institute of Food, Nutrition and Health, ETH Zurich, Zürich, Switzerland.

³Agroscope, Plant Pathology and Zoology in Fruit and Vegetable Production, Wädenswil, Switzerland.

Summary

Bacteriophages are highly selective in targeting bacteria. This selectivity relies on the specific adsorption of phages to the host cell surface. In this study, a Tn5 transposon mutant library of *Erwinia amylovora*, the causative agent of fire blight, was screened to identify bacterial receptors required for infection by the podovirus S6. Phage S6 was unable to infect mutants with defects in the bacterial cellulose synthase operon (*bcs*). The Bcs complex produces and secretes bacterial cellulose, an extracellular polysaccharide associated with bacterial biofilms. Deletion of the *bcs* operon or associated genes (*bcsA*, *bcsC* and *bcsZ*) verified the crucial role of bacterial cellulose for S6 infection. Application of the cellulose binding dye Congo Red blocked infection by S6. We demonstrate that infective S6 virions degraded cellulose and that Gp95, a phage-encoded cellulase, is involved to catalyse the reaction. In planta S6 did not significantly inhibit fire blight symptom development. Moreover, deletion of *bcs* genes in *E. amylovora* did not affect bacterial virulence in blossom infections, indicating that sole application of cellulose targeting phages is less appropriate to biologically control *E. amylovora*. The interplay between cellulose synthesis, host cell infection and maintenance of the host cell population is discussed.

Received 17 December, 2021; revised 3 March, 2022; accepted 7 March, 2022. *For correspondence. E-mail lars.fieseler@zhaw.ch; Tel: +41 58 934 54 07. †Present address: Microeos AG, Wädenswil, Switzerland. ‡Present address: Unilabs AG, Dübendorf, Switzerland. #Present address: Lonza AG, Visp, Switzerland.

Introduction

Bacteriophages are viruses that exclusively infect bacteria. These natural predators pose the most abundant biological entity on earth, reaching an estimated number of 10^{31} (Casjens, 2005; Hatfull, 2008; Cobián Güemes *et al.*, 2016), and outnumber bacteria by at least 10-fold (Brüssow and Hendrix, 2002). Because of their unique properties phages are becoming an attractive alternative to antibiotics (Al-Ishaq *et al.*, 2020).

Phages recognize hosts through receptors on their surface. In Gram-negative bacteria, these receptors can be outer membrane proteins (Marti *et al.*, 2013), carbohydrate moieties of lipopolysaccharides (LPS), exopolysaccharides and capsular polysaccharides (Fehmel *et al.*, 1975), or other cell surface structures located in appendages such as pili (Guerrero-Ferreira *et al.*, 2011) and flagella (Shin *et al.*, 2012; Bertozzi Silva *et al.*, 2016). The adsorption is highly specific for a particular phage. A phage can therefore only infect bacterial strains or serotypes depending on the presence of its receptor. In general, binding of a particular receptor through a phage tail fibre or tail spike protein represents the first interaction between a phage and a host cell. To minimize accessibility of a receptor, bacteria can cover these structures with secreted exopolysaccharides, capsular polysaccharides or by establishing a biofilm (Labrie *et al.*, 2010). Phages, however, have developed mechanisms to interact with these physical barriers. An increasing number of phages were observed to encode depolymerases in their genomes. These enzymes are highly efficient in degrading such extracellular polysaccharides. Pires *et al.* (2016) analysed the function of 160 predicted depolymerases by 143 different phages. Phage encoded depolymerases have been shown to be specific for different substrates such as sialic acid, levan, amylovan, xylan, dextran, rhamnogalacturonan, hyaluronate, LPS, alginate or pectin (Born *et al.*, 2014; Pires *et al.*, 2016). An extensive overview of the identified and characterized depolymerases can be found in previously published reviews (Pires *et al.*, 2016; Latka *et al.*, 2017, 2019; Knecht *et al.*, 2020). By degrading these polysaccharides, depolymerases enhance and

facilitate the accessibility of the bacterial surface. The K-type specific phages of *Klebsiella aerogenes* and *Acinetobacter baumannii* and the *Erwinia amylovora* phage L1 even depend on these barriers for successful infection (Hsu *et al.*, 2013; Born *et al.*, 2014; Lin *et al.*, 2014; Hsieh *et al.*, 2017; Oliveira *et al.*, 2017, 2019; Pan *et al.*, 2017).

Bacteriophage S6 (HQ728266), a member of the *Schitoviridae* family, was isolated from Swiss apple and pear orchards in 2011 (Born *et al.*, 2011). It encodes a putative virion-encapsidated RNA polymerase, a hallmark of N4-like phages (Kazmierczak and Rothman-Denes, 2006). Phage S6 is strictly lytic and highly specific for *E. amylovora* and was therefore regarded as a promising biocontrol agent. It seems that the pathogen can be best controlled by combinations of different phages (Born *et al.*, 2011). In such 'phage cocktails' each phage should ideally recognize a different receptor on the host cell surface. However, with the exception of the amylovoran specific phage L1 (Born *et al.*, 2014), receptors of *E. amylovora* specific phages have not been determined yet.

The Gram-negative, facultative anaerobe *E. amylovora* is the causative agent of fire blight (Bonn and van der Zwet, 2000; Vanneste, 2000). This serious plant disease affects members of the *Rosaceae* family and is one of the 10 most devastating plant pathogens in crop production (Momol and Aldwinckle, 2000; Thomson, 2000; Gill *et al.*, 2003; Mansfield *et al.*, 2012). *Erwinia amylovora* infects blossoms, enters the plant tissue and forms biofilms that clog the xylem vessels (Geider, 2000; Vanneste and Eden-Green, 2000; Wei *et al.*, 2000; Koczan *et al.*, 2011; Castiblanco and Sundin, 2016). This leads to desiccation of infected tissues resulting in the characteristic disease symptoms (Vanneste and Eden-Green, 2000). Essential for the high pathogenicity of *E. amylovora* is the secreted exopolysaccharide amylovoran (Ayers *et al.*, 1979; Bereswill and Geider, 1997; Maes *et al.*, 2001; Koczan *et al.*, 2009). Aside from amylovoran and levan, bacterial cellulose (BC) was found to be produced by *E. amylovora* during the infection of susceptible plant tissues (Castiblanco and Sundin, 2016). Castiblanco and Sundin (2016) proposed that BC synthesis is critical to form a mature biofilm, in order to withstand disturbances generated by the xylem-sap flow. Both amylovoran and biofilm formation are tightly regulated by the intracellular second messenger cyclic-di-GMP (c-di-GMP) (Edmunds *et al.*, 2013; Castiblanco and Sundin, 2016; Kharadi *et al.*, 2019).

The aim of this study was to examine the interaction between S6 and its host. We show that BC is a key component for successful infection of *E. amylovora* by S6 and we provide evidence that S6 harbours an enzymatically active cellulase. Host cells lacking BC synthesis

were not infected by S6 and were not attenuated during blossom infections.

Results

Bacteriophage S6 cannot infect host cells lacking bacterial cellulose

A Tn5 transposon mutant library of *E. amylovora* CFBP 1430 was screened for S6 resistant mutants. Tn5 insertion mutants of the *bcs* operon exhibited resistance against S6 infection (data not shown). S6 resistant mutants revealed insertions in the genes *bcsO*, *bcsQ*, *bcsA*, *bcsB*, *bcsC* and *bcsZ*. The only gene in this operon not disrupted by the transposon was *bcsD* (Fig. 1A). In addition to the *bcs* operon, S6 was unable to infect a mutant with a disrupted *hmsT* gene (data not shown). This gene is not located in the *bcs* operon and is annotated as a diguanylate cyclase which could be involved in the production of c-di-GMP, a second messenger that induces cellulose production (Edmunds *et al.*, 2013). All genes but *hmsT* were disrupted multiple times at independent sites in different mutants, reducing the risk of insertion bias (Fig. 1A). The operon is composed of seven genes encoding different subunits of the BC synthase complex, which is required for the production and secretion of BC (Omadjela *et al.*, 2013). Located in the inner membrane, the catalytically active subunit BcsA contains a large glycosyltransferase domain, generating β -1,4-glycosidic linkages (Omadjela *et al.*, 2013). BcsB is co-localized with BcsA to stabilize the complex (Morgan *et al.*, 2013). Cellulose strands are crystallized by the periplasmic protein BcsD and exported by the outer membrane protein BcsC (Whitney *et al.*, 2011; Römling and Galperin, 2015). The *bcsZ* gene (annotated as *celA3*) encodes a putative endoglucanase and is involved in cellulose regulation (Castiblanco and Sundin, 2016). Essential for cellulose production are the subunits BcsQ, BcsA, BcsB, BcsC and BcsZ (Le Quéré and Ghigo, 2009). Figure 1B illustrates the composition of the Bcs complex schematically.

Based on these findings, clean knockout mutants were generated. A gene potentially involved in phage attachment is *bcsC* since the encoded protein is embedded in the outer membrane where it could be targeted by S6 ($\Delta bcsC$). To establish if S6 requires BC for infection, a deletion of the catalytic subunit BcsA ($\Delta bcsA$) and a *bcsZ* knockout ($\Delta bcsZ$) were generated. Additionally, the complete *bcs* operon was deleted (Δbcs). Western blots, using polyclonal Anti-BcsC antibodies, were carried out to confirm the presence or absence of BcsC in the mutants (data not shown). The deletions of *bcsA*, *bcsC*, *bcsZ* or the entire operon rendered all mutants phage-insensitive. When arabinose was used to induce protein

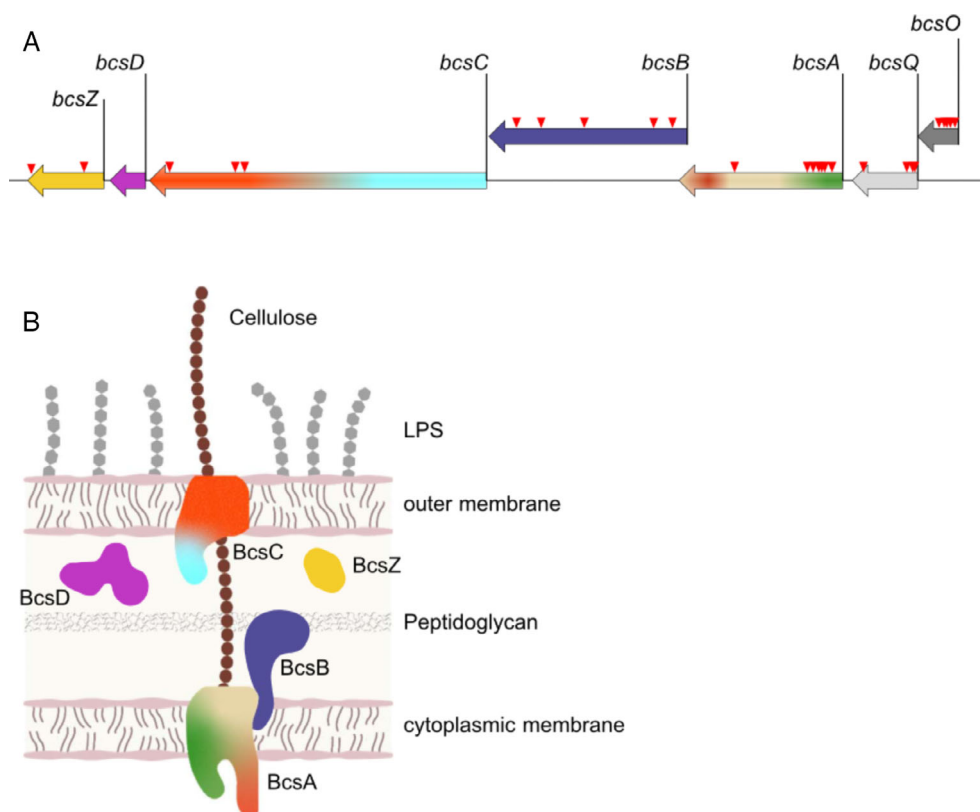


Fig. 1. Schematic overview of the bacterial cellulose synthase operon (*bcs*).

A. Overview of the *bcs* operon in *E. amylovora* CFBP 1430. Red arrows indicate independent Tn5 insertion events identified in phage S6 resistant mutants.

B. Predicted localization of the encoded Bcs components in the cell wall of *E. amylovora*. BcsA: putative glycosyltransferase located in the inner membrane; BcsB, BcsD and BcsZ: putative periplasmic proteins, BcsZ: endoglucanase; BcsC: outer membrane protein for cellulose export; brown circles: bacterial cellulose; LPS: lipopolysaccharide.

expression *bcsA* and *bcsC* complemented mutants ($\Delta bcsA + bcsA$ and $\Delta bcsC + bcsC$) were successfully infected and lysed by S6. However, plaques of S6 on the complemented mutants were not as clear as on the wild type. The complemented *bcsZ* mutant ($\Delta bcsZ + bcsZ$) remained insensitive to S6 infection (Fig. 2). Complementing the mutant Δbcs with *bcsC* ($\Delta bcs + bcsC$) could not restore phage sensitivity indicating that S6 interacts with BC. The *hmsT* gene was not investigated further, as the potentially produced secondary messenger can have manifold effects on cell metabolism and behaviour. However, it seems that overexpression of *hmsT* did not inhibit phage infection.

Congo Red blocks S6 infection of *E. amylovora*

The BC synthase complex is responsible for cellulose production. Hence, the mutants' ability to produce BC was tested using Congo Red, a dye that binds to 1,4- β -glucose polymers (Carder, 1986). BC producing strains grew as pink colonies, whereas cells lacking cellulose appeared as white colonies (Fig. 3). Mutants lacking the

enzymatically active subunit BcsA were unable to produce BC and thus appeared as white colonies. The *bcsC* knockout mutant grew as light rose-coloured colonies. As the cellulose producing subunit BcsA is present, cellulose is produced but not secreted in the absence of BcsC. $\Delta bcsZ$ colonies also appeared to be light pink. Complementations of the knock-out mutants were also evaluated. When protein production was induced, the pink colony morphology could be restored. An exception was Δbcs complemented with *bcsC* where the enzymatic active subunit BcsA was still missing and the complemented *bcsZ* mutant ($\Delta bcsZ + bcsZ$), which remained light pink (Fig. 3).

In addition, phage dilutions were spotted on a wild type bacterial lawn on LB plates supplemented with Congo Red. In contrast to the controls, S6 was unable to infect the bacteria (Fig. 4). When Congo Red was added at lower concentrations, the effect was less pronounced. To verify if Congo Red generally blocks phage infection by unspecifically binding to surface structures that would obstruct host receptor binding, the phages L1 (*Autographiviridae*) and Y2 (*Chaseviridae*) were used as

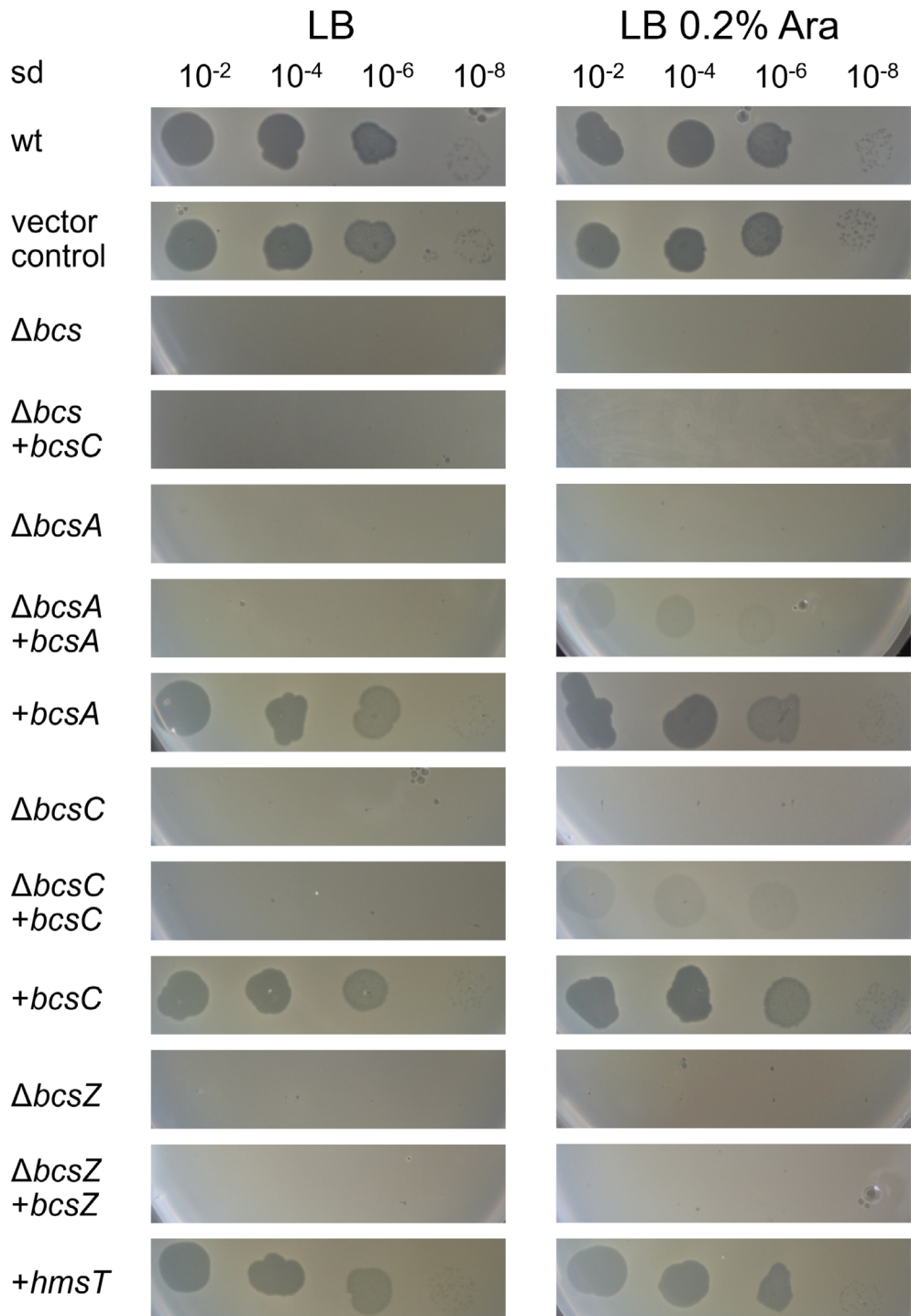


Fig. 2. Plaque assay of phage S6. Serial dilutions (sd) of phage S6 were spotted onto *bcs* mutant lawns on Luria agar (LB) with and without the addition of 0.2% (wt./vol.) arabinose (Ara) as an inducer of protein expression to verify infection. Deletions of *bcsA*, *bcsC*, *bcsZ* or the entire *bcs* operon rendered all mutants phage-insensitive. After complementation ($\Delta bcsA + bcsA$ and $\Delta bcsC + bcsC$) only faint plaques of S6 were observed. wt: wild type.

negative controls. Neither L1 nor Y2 supposedly recognizing amylovoran or LPS respectively (Born *et al.*, 2014; Born *et al.*, 2017), were affected by the dye. In liquid

culture the addition of S6 to the wild type led to a delayed growth of 5 h before an increase of the OD_{600nm} was detectable. This delaying effect was eliminated when

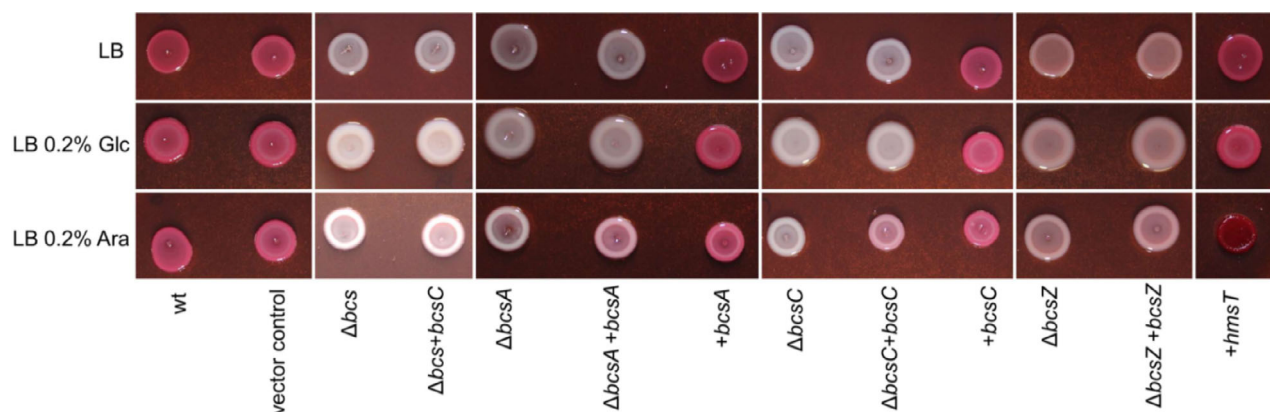


Fig. 3. Cellulose production of *bcs* mutants. Cellulose production was monitored using Congo Red added to the medium. Five microliters overnight culture of *E. amylovora* CFBP 1430 (wt) and each *bcs* mutant were spotted on Luria agar plates (LB) with Congo Red and Coomassie Brilliant Blue only or amended with 0.2% (wt./vol.) glucose (Glc) or arabinose (Ara, inducer of protein expression). BC producing strains grow with a pink phenotype, whereas cellulose-lacking strains grow as white colonies.

Congo Red was added, suggesting a loss of S6 infectivity. Growth of the Δbcs mutant was unaffected by both, phage and Congo Red supplementation. Notably in the absence of S6 Congo Red delayed exponential growth of wild type bacteria ca. 2–3 h. In the absence of Congo Red cellulose, negative strains exhibited the same delay, e.g. a slightly longer lag phase (data not shown). To verify if Congo Red affects the virion, S6 was recovered after the experiment, washed, and a dilution row was spotted on an *E. amylovora* wild type lawn on Luria agar. S6 infected the wild type indicating no effect of Congo Red on the virion. These results indicate that Congo Red blocks S6 infection by binding to cellulose.

Bacteriophage S6 encodes a functional cellulase

To study the interaction of S6 with BC, the phage's ability to degrade amorphous cellulose (CMC) was tested. Purified phage stocks were incubated directly with cellulose to observe enzyme activity. The phages L1 and Y2 were used as negative controls. The cellulase from *Trichoderma reesei* was used as positive control. In this experiment phage, S6 was able to degrade cellulose to glucose molecules (Fig. 5).

Genome analysis revealed that S6 has low sequence coverage with close relatives in the ORF's encoding the putative tail structure. Gp94, Gp95 and Gp96 seem to encode proteins with potential cellulolytic abilities. A phylogenetic analysis was carried out to investigate this hypothesis (data not shown). Proteins sharing high sequence identity with Gp94, Gp95 and Gp96 were identified through an NCBI BLAST search. The phylogenetic analysis of the phage-encoded proteins clusters Gp94 and Gp95 with proteins annotated as 1,4- β -cellobiosidases (Gp94) or putative endoglucanases (Gp95). Gp96 does not cluster with any of the

investigated proteins reflecting the overall poor sequence identity of Gp96 with other proteins. In contrast to the other two proteins, Gp96 does not harbour any known enzymatic or structural domain. The C-terminal part of Gp96 does not share similarities with other proteins found in the NCBI GenBank database. The N-terminal part, however, shares similarities with other phage proteins. Especially the amino acid section 10-39 of Gp96 has a $\geq 50\%$ identity to the N-terminal region of other N4-like phage proteins. The proteins of *E. amylovora* phages Frozen (Gp95), Gutmeister (Gp87), Rexella (Gp94) and Ea9-2 (Gp85) all share 50% sequence homology and *E. coli* phage Pollock (Gp76; 53.33%), *Salmonella* phage FSL SP-058 (SP058_00390; 56.67%), *Salmonella* phage FSL SP-076 (SP076_00305; 56.67%) and *Enterobacter* phage EcP1 (Gp64; 56.67%) even share a higher sequence identity. Most of these proteins have been annotated as tail spikes or tail fibre proteins.

Bioinformatics showed that Gp94 harbours two separate domains. The Calx-beta domain located at the N-terminus forms self-contained beta sheets (Alonso-García *et al.*, 2009). Structure prediction by SWIS-SMODEL (Waterhouse *et al.*, 2018) indicates that this domain protrudes from the protein. It is reasonable to speculate that this domain could be involved in attaching the protein to the phage particle. The C-terminal part of Gp94 contains a glycosyl hydrolase (family 48) domain. Members of this family are endo- or exoglucanases that cleave cellulose (Myers and Northcote, 1959; Datta *et al.*, 1963; Halliwell *et al.*, 1972; Berghem and Pettersson, 1973; Eriksson and Pettersson, 1975).

In silico analysis of Gp95 revealed a C-terminal part, which spans approximately 325 amino acids (The UniProt Consortium, 2019), HHpred (Zimmermann *et al.*, 2018)] and forms a glycoside hydrolase (family 5) domain. This domain supposedly mediates the enzymatic

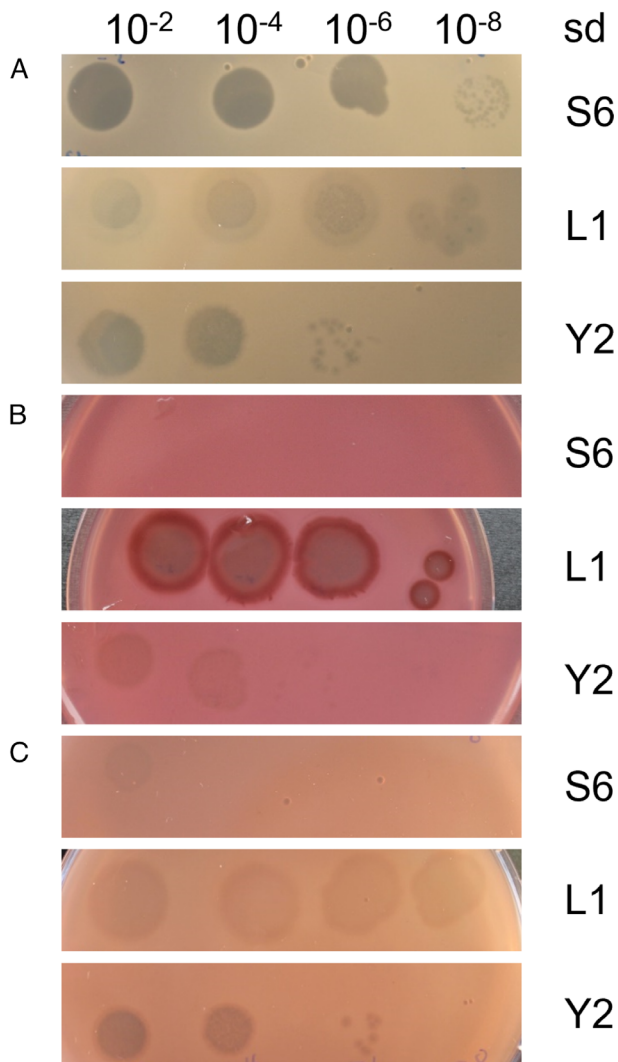


Fig. 4. Dose-dependent Congo Red protection against infection by phage S6. Serial dilutions (sd) of phage S6 were spotted onto Luria soft agar overlays containing *E. amylovora* CFBP 1430. A: Luria agar, B: Luria agar amended with $40 \mu\text{g ml}^{-1}$ Congo Red and $20 \mu\text{g ml}^{-1}$ Coomassie Brilliant Blue, C: Luria agar amended with $20 \mu\text{g ml}^{-1}$ Congo Red and $10 \mu\text{g ml}^{-1}$ Coomassie Brilliant Blue. The *E. amylovora* specific podovirus L1 and the myovirus Y2 were used as controls.

function, as several family members were shown to have an enzymatic function as cellulases, endo- β -1,4-glucanases, endo- β -1,4-xylanases, or β -mannosidases respectively (Aspeborg *et al.*, 2012).

Different concentrations of purified Gp94 and Gp95 proteins were analysed for cellulase activity at different temperatures. Only Gp95 showed enzymatic activity under the tested conditions. The protein exhibited high activity and stability at temperatures ranging from 25°C up to 70°C with the highest enzymatic activity at 40°C . This aligns well with the finding that the highest release of glucose for incubations with entire S6 virions was observed at 50°C (Fig. 6A). Compared to the cellulase of

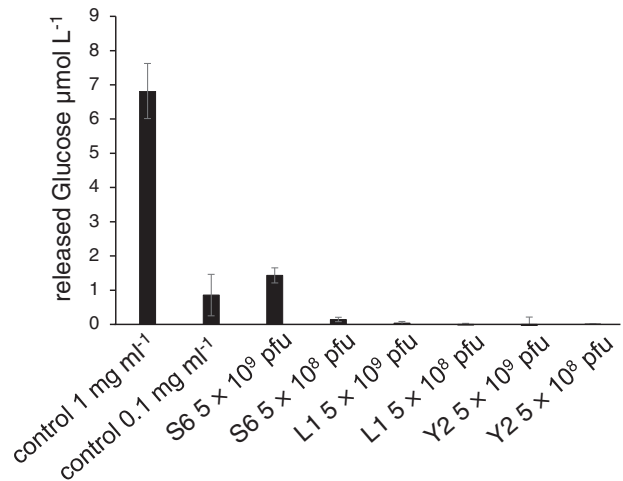


Fig. 5. Cellulase activity of whole S6 virions. The amount of released glucose after digestion of carboxymethyl cellulose (CMC) by phage S6 was measured using the colorimetric shift of dinitrosalicylic acid solution (DNS) upon encounter of reducing sugars. The cellulase of *Trichoderma reesei* (0.2 units; 0.02 units) was used as positive control, the two phages L1 and Y2 as negative controls since neither of the two phages encode cellulases. Error bars indicate the standard deviation of three independent experiments. pfu: plaque-forming units.

Trichoderma reesei, which was used as a positive control, Gp95 seems to be more active at 40°C (Fig. 6B).

Lack of cellulose synthesis does not attenuate *E. amylovora* virulence on detached flowers

Because BC is a constituent of *E. amylovora* EPS, possible effects of Δbcs , $\Delta bcsA$, $\Delta bcsD$ and $\Delta bcsZ$ mutations on the production of amylovoran in *E. amylovora* were evaluated by amylovoran-CPC precipitations (Bellemann *et al.*, 1994). The low EPS producing strain 4/82 was used as negative control (Born *et al.*, 2014), along with CFBP1430 which served as positive control. A vector control was also added. The generated deletion mutants Δbcs , $\Delta bcsA$, $\Delta bcsC$ and $\Delta bcsZ$, the complemented mutants $\Delta bcs + bcsC$, $\Delta bcsA + bcsA$, $\Delta bcsC + bcsC$, and $\Delta bcsZ + bcsZ$, and *hmsT*-, *bcsA*- and *bcsC*- over-expressing mutants revealed similar levels of amylovoran as the positive controls (Fig. 7). These findings suggest that modifications in the *bcs* operon do not affect production of amylovoran in *E. amylovora*.

Virulence of the generated knockout mutants was tested for variation on detached blossoms. Wild type bacteria of CFBP 1430 and the strain carrying the empty vector were used as positive controls. Both strains were potent in infecting the blossoms and generated overall 91% and 92% grade 3 disease symptoms (infection symptoms visible in the blossoms and stipe) respectively. Comparable results were obtained when blossoms were

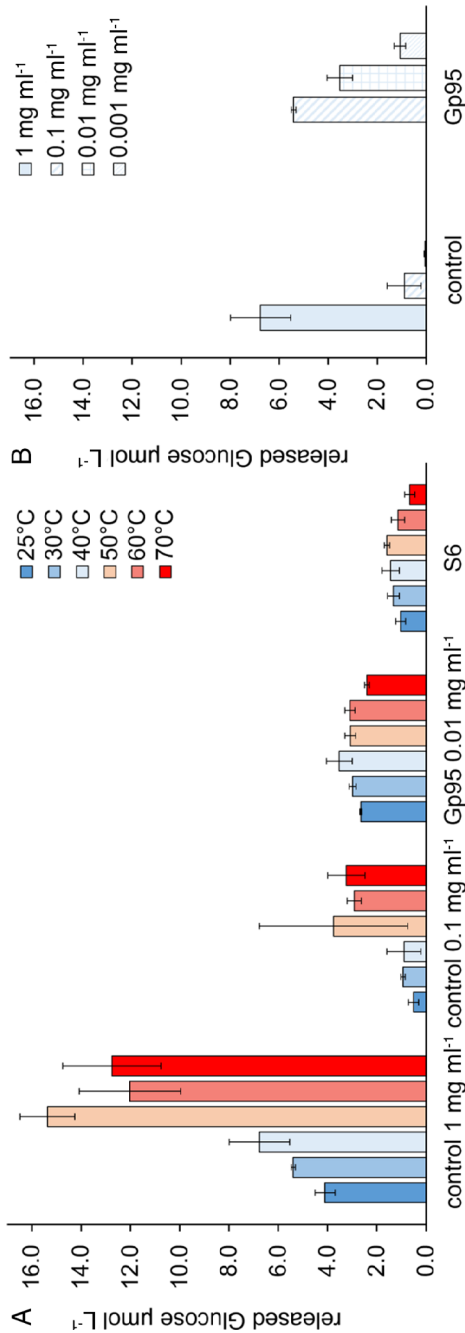


Fig. 6. Cellulase activity of Gp95. The total amount of released glucose after carboxymethyl cellulose digestion by the phage cellulase Gp95 was measured using the colorimetric shift of dinitrosalicylic acid solution (DNS) upon encounter of reducing sugars. The cellulase of *Trichoderma reesei* was used as positive control.

A. Temperature-dependent activity of Gp95. B. Concentration-dependent activity of Gp95 was measured at 40 °C. Error bars indicated the standard deviation of at least three independent experiments.

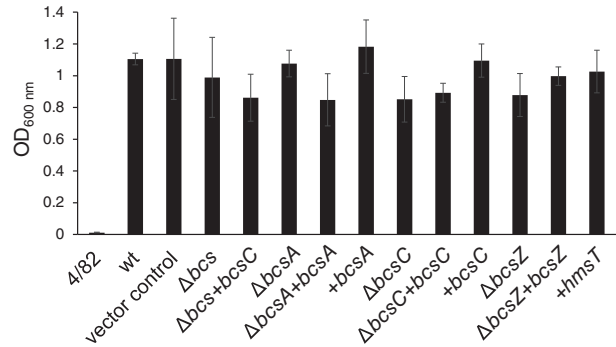


Fig. 7. Amylovoran production in *E. amylovora* CFBP 1430 (wt) and isogenic *bcs* mutants. Optical density of amylovoran CPC precipitation was measured at 600 nm. The low EPS producing strain *E. amylovora* 4/82 was used as negative control. Each experiment was carried out three times for each strain. Error bars indicate standard deviation.

infected with Δbcs , $\Delta bcs + bcsC$, $\Delta bcsA$, $\Delta bcsA + bcsA$, $\Delta bcsC$ and $\Delta bcsC + bcsC$. The infection with the two mutants $\Delta bcsZ$ and $\Delta bcsZ + bcsZ$ generated less grade 3 disease symptoms on infected blossoms namely, 66% and 72% respectively. The over-expression of *hmsT*, which positively regulates the BC synthase through c-di-GMP production, generated 88% of grade 3 blossoms when applied (data not shown). These findings indicate that virulence on detached flowers is not significantly affected by the modifications in the *bcs* operon.

Detached flowers were also applied to monitor the bio-control efficacy of S6. In this experiment infection by *E. amylovora* revealed 70% grade 3 disease symptoms in the untreated control. Application of S6 to artificially contaminated blossoms did not reveal significant differences in disease symptoms compared to the positive control indicating that S6 alone cannot be used to treat blossom infections by *E. amylovora* (data not shown).

Discussion

In this study, a Tn5 mutant library was screened to discover surface structures interacting with phage S6 during infection. The localization of the Tn5 insertions revealed mutants with disruptions in the *bcs* operon. Gene deletion and complementation analysis confirmed that S6 could not infect mutants impaired in the production of BC. Interestingly, insensitivity against S6 infection of the $\Delta bcsZ$ mutant could not be restored after complementation. BcsZ can have different effects on cellulose production. In *E. coli* (Mazur and Zimmer, 2011), *Salmonella* (Ahmad *et al.*, 2016), *Serratia* (An *et al.*, 2022), *Herbaspirillum rubrisubalbicans* (Tuleski *et al.*, 2019) and *Komagataeibacter xylinus* (formerly known as *Acetobacter xylinum*) (Koo *et al.*, 1998) BcsZ exhibits

endo- β -1,4-glucanase activity and is needed for cellulose production. In *E. amylovora* BcsZ is also necessary for c-di-GMP regulation of cellulose biosynthesis (Castiblanco and Sundin, 2016). Insensitivity against S6 infection in the $\Delta bcsZ$ mutant can be explained by the lack of BC production. Overexpression of *bcsZ* might also affect cellulose biosynthesis thereby preventing S6 infection. However, further research is required to demonstrate regulation of cellulose production by BcsZ.

The interaction of BC and S6 was monitored with the cellulose-binding dye Congo Red. The dye appears to have a concentration-dependent blocking effect on S6, since infection of the host could be completely abolished. Additionally, S6 virions were able to digest cellulose. Proteins that could be responsible for this activity, namely Gp94, a putative 1,4- β -cellobiosidase, and Gp95, a putative endoglucanase, were further analysed. Despite the promising *in silico* data for Gp94, we could not detect enzymatic activity against CMC or cellobiose (data not shown). Purification of Gp94 was challenging, as most of the protein was insoluble which might have affected the enzymatic activity. Gp95 showed enzymatic activity and can be accounted for the observed cellulase activity of phage S6 virions. The protein exhibited high thermostability and could be stored at 4°C for more than 6 months without loss of function (data not shown). Compared to the *Trichoderma reesei* cellulase, Gp95 revealed a higher activity. However, this may also be due to the experimental conditions, which were optimized for Gp95.

Gp95 is likely attached to the phage particle. To ensure integration into the virion, depolymerases may use different linker systems (Knecht et al., 2020). Phage N4, a close relative of S6, links its receptor-binding protein Gp66 via the N-terminal region to its tail (Prokhorov et al., 2017). G7C, another N4-like virus, also uses this N-terminal domain to attach its depolymerase Gp66 to G7C particles. This protein holds a further branching domain (similar to the Gp10_{T4} domain) which allows binding of additional proteins (Broeker and Barbirtz, 2017; Prokhorov et al., 2017). Gp95 contains two choice-of-anchor D domains at the N-terminus with unknown function. We hypothesize that this region might be involved in attaching the cellulase to the phage particle. However, at this point, it cannot be confirmed that Gp95 forms a structural protein of S6.

Many phages use mucous layers as receptors (Lindberg, 1973; Rakhuba et al., 2010; Born et al., 2014; Bertozzi Silva et al., 2016). S6 may either use BC directly as a receptor or could reach the bacterial surface more easily by decomposing the cellulose layers, thereby weakening the integrity of the capsule. A preference analysis of *Caudovirales* for receptor types revealed that Podoviruses as S6 bind mainly to polysaccharides (Bertozzi Silva

et al., 2016). Although the number of analysed phage-receptor pairs was comparatively small, the exclusivity of podoviruses to bind to polysaccharides is striking. Roach et al. investigated the impact of EPS in *E. amylovora* on phage infection. Myoviruses appeared to be better adapted for low EPS producing strains, whereas podoviruses were highly infectious towards high EPS producing hosts (Roach et al., 2013). Considering these results, and the fact that S6 harbours an enzymatically active cellulase, indicates that S6 recognizes BC and relies on it for infection. The identification of phage-encoded cellulases substantiates the crucial role of BC in the S6 infection process.

In vitro S6 seems to stabilize bacterial growth instead of rapidly eradicating the host (Born et al., 2011). Infection experiments using detached flowers revealed similar results. Hence, S6 is not capable of biocontrolling *E. amylovora*. Fujiwara et al. (2011) obtained similar findings for *Ralstonia solanacearum* phage RSL1. Instead of quickly killing their hosts, RSL1 kept the cell density at a low level, maintaining a host-phage coexistence. S6 might establish such an equilibrium between bacterial growth and host lysis. Considering the importance of BC for S6 infection, we hypothesize that BC production might be relevant for the observed coexistence. BC synthesis is tightly controlled and upregulated in the presence of high cell counts (Bai and Rai, 2011; Lamas et al., 2016). High bacterial density will initiate cellulose secretion upon which S6 is able to attack. This process will inevitably reduce the number of host cells, thereby halting cellulose production in the surviving population. Because S6 exhibits a relatively long latency period of 110 min in laboratory settings (Supplementary Fig. 1) non-infected bacteria would be able to adapt and re-grow without producing BC. A temporary loss of BC production will not affect virulence of the host during blossom infection. In the absence of cellulose, S6 is unable to recognize the host which would permit a recovery of the bacterial population until the cycle starts anew. This scenario could explain coexistence of the virulent S6 phage and its host cells. Our study underlines the importance to identify phage receptors and to decipher the function of phage-encoded depolymerases for a better understanding of the phage infection process and the efficacy in controlling bacterial populations.

Experimental procedures

Culture condition

Bacteria were cultivated in Luria broth and on Luria agar (10 g L⁻¹ tryptone, 10 g L⁻¹ NaCl, 5 g L⁻¹ yeast extract, with or without the addition of 15 g L⁻¹ agar, Laboratorios Conda S. A, Spain) at 28°C (*E. amylovora*), or 37°C (*Escherichia*

coli) (Supplementary Table 1). The antibiotics kanamycin ($50 \mu\text{g ml}^{-1}$), streptomycin ($100 \mu\text{g ml}^{-1}$) and ampicillin ($100 \mu\text{g ml}^{-1}$) were added if required.

Bacteriophage propagation and purification

S6 was propagated using the soft agar overlay method (Supplementary Table 1) (Adams, 1959). Four milliliters of molten Luria soft agar (10 g L^{-1} tryptone, 10 g L^{-1} NaCl, 5 g L^{-1} yeast extract, 4 g L^{-1} agar, with the addition of 2 mM MgSO_4 , 10 mM CaCl_2) was supplemented with $90 \mu\text{l}$ bacterial overnight culture and $10 \mu\text{l}$ diluted bacteriophage and spread on Luria agar plates to generate semi confluent lysed plates. After overnight incubation, 5 ml SM buffer (100 mM NaCl , 8 mM MgSO_4 , 50 mM Tris-Cl , pH 7.4) was added per plate and incubated for 5 h at room temperature (RT) with shaking. Phages were precipitated from the supernatant using polyethylene glycol (10% (wt./vol.) PEG 8000, 0.5 M NaCl ; ice bath at 4°C , overnight) and pelletized (10 min , $10\,000\text{g}$), and the pellet was re-suspended in 5 ml SM buffer . Phages were purified using CsCl gradient centrifugation (Sambrook and Russell, 2001) and dialyzed against SM buffer (6 h , RT).

Transposon mutagenesis and screening of phage resistant mutants

To generate electrocompetent cells, an overnight culture of *E. amylovora* CFBP 1430 was diluted 1:1000 and incubated with shaking until an optical density of 0.5 was reached at 600 nm wavelength ($\text{OD}_{600\text{nm}}$). Cells were placed on ice for 30 min . Using ice-cold 5% (vol./vol.) glycerol, the cells were washed three times before re-suspending in 10% (vol./vol.) glycerol. Cells were kept at -80°C until further use. To generate the transposon mutants, $40 \mu\text{l}$ of electrocompetent cells were supplemented with $1 \mu\text{l}$ of a transposome (EZ-Tn5 <KAN2> Tnp; Epicenter, Madison, USA) and electroporated (25 V , $25 \mu\text{F}$, 200Ω). Immediately after electroporation, the cells were re-suspended in 4 ml SOC medium [2% (wt./vol.) tryptone, 0.5% (wt./vol.) yeast extract, 10 mM NaCl , 2.5 mM KCl , 10 mM MgCl_2 , 10 mM MgSO_4 and 20 mM glucose] (Hanahan, 1983) and incubated for 3–4 h at 28°C with shaking. The suspension was serially diluted and plated on kanamycin containing Luria agar plates. Single colonies were picked and stored in 96-well plates filled with Luria broth amended with 10% (vol./vol.) glycerol at -86°C .

To identify phage resistant mutants, liquid cultures of the transposon library were prepared in 96-well plates filled with Luria broth amended with kanamycin ($25 \mu\text{g ml}^{-1}$) using a 96-well replica plater (Merck, Switzerland) and incubated at 28°C overnight. The next

day molten Luria soft agar containing kanamycin ($25 \mu\text{g ml}^{-1}$) and 5% (vol./vol.) glycerol was prepared. One batch was amended with S6 (10^5 PFU ml^{-1}), the other was used without phages. Each soft agar was distributed into 96-well flat-bottom plates, $200 \mu\text{l}$ per well. Immediately after distribution, the bacterial cultures of the transposon library were transferred into the prepared soft agar plate using the 96-well replica plater. The plates were incubated overnight at 25°C for optimal phage infection and the $\text{OD}_{600\text{nm}}$ of each well was measured using a Synergy H1 Multi-Mode Microplate Reader (BioTek Instruments). The $\text{OD}_{600\text{nm}}$ of cultures grown in the presence of S6 was subtracted from the $\text{OD}_{600\text{nm}}$ of cultures grown in the absence of S6. A resulting difference $\Delta \text{OD}_{600\text{nm}} \leq 0.15$ was defined to identify phage resistant mutants. Then transposon mutants resistant to phage infection were confirmed to resist plaque formation by S6 using the standard soft agar overlay method (Adams, 1959).

Arbitrary-primed PCR as described by Das *et al.* (2005) was performed to identify transposon insertion sites (Das *et al.*, 2005). Arbitrary primers Arb-P1, Arb-P2 and Arb-P3 (Supplementary Table 2) were paired with the nested primer 1. Using the purified PCR product as template, a second PCR was performed with the anchor primer and the nested primer 2. The amplified shorter product was purified and sequenced (Microsynth, Switzerland). The sequences were aligned to the *E. amylovora* CFBP 1430 genome (FN434113) to locate the transposon insertion site.

Generation of mutants

The Tn5 library screen revealed that gene disruptions in the BC synthase operon *bcs* render *E. amylovora* CFBP 1430 phage resistant. To elucidate the impact of the *bcs* operon on S6, the genes *bcsA*, *bcsC* and *bcsZ* were replaced by a kanamycin resistance gene. Knockout mutants were generated by allelic exchange using the suicide plasmid pKAS32 carrying an R6K origin of replication (Supplementary Table 2) (Skorupski and Taylor, 1996). Flanking regions of the gene of interest (ca. 1 kb in length) and a kanamycin cassette (*aph7*) amplified from pSB315 (Galán *et al.*, 1992) were ligated into the multiple cloning site of pKAS32. The fragments were amplified using Gibson assembly primers designed by the NEBuilder tool (NEBuilder Assembly Tool v1.12.18) using the KAPA HIFI™ PCR kit (KAPA Biosystems, Wilmington, USA) (Supplementary Table 2). The vector pKAS32 was extracted from *E. coli* S17-1 λpir [pKAS32] according to the NucleoSpin® Plasmid Kit by Macherey-Nagel (Düren, Germany). The vector pKAS32 was linearized by EcoRV (37°C , 1 h). The product was

analysed by electrophoresis and purified from a 1% (wt./vol.) agarose gel by the DNA Clean & Concentrator™-5 Kit (Zymo Research). To prevent re-circularization of the linearized vector, a dephosphorylation step was carried out (CIP, 1 U/250 ng vector). The plasmid was purified and eluted in 15 µl ultrapure H₂O (Satorius, Germany). The insert was phosphorylated to facilitate formation of the vector. The suicide plasmid was generated either through Gibson assembly (Gibson *et al.*, 2009) or through classic ligation using a T4 polynucleotide ligase (Thermo Fisher Scientific) according to the manufacturer's protocol. The plasmids were introduced into electrocompetent, streptomycin-resistant *E. amylovora* CFBP 1430 by electroporation. After electroporation, the cells were re-suspended in SOC medium and incubated at 30°C for 1 h with vigorous shaking. Subsequently, the cells were plated on Luria agar plates complemented with kanamycin and streptomycin. Correctness of deletion was verified by PCR.

The arabinose inducible plasmid pBAD18 (Guzman *et al.*, 1995) holding an ampicillin resistance was linearized with EcoRI and HindIII (37°C, 1 h) and purified. The inserts and their ribosomal binding sites were amplified from *E. amylovora* CFBP 1430 by PCR with Gibson primers (NEB). PCR products with the correct length were recovered from a 1% (wt./vol.) agarose gel. The linearized vector pBAD18 and the insert were joined by Gibson assembly (Gibson *et al.*, 2009). The newly formed plasmids were introduced into electrocompetent *E. coli* XL1-Blue cells for amplification. Cells were recovered in SOC and incubated for 1 h at 37°C with vigorous shaking before plating onto Luria agar plates containing ampicillin. Correct plasmid insertion was verified by PCR with the primer pair pBAD fw and pBAD rev (Supplementary Table 2). Correct plasmids were extracted and introduced into electrocompetent *E. amylovora* CFBP 1430, the generated knockout mutants. Plaque assays involving different dilutions of S6 were carried out and the plaque-forming ability was monitored. Luria soft agar and Luria agar plates were amended with 100 µg ml⁻¹ ampicillin and 0.2% (wt./vol.) arabinose for promoter induction or 0.2% (wt./vol.) glucose for promoter repression.

Growth curve

The impact of the generated gene modifications on the growth of these mutants was monitored. Bacteria were washed twice in Luria broth and OD_{600nm} was adjusted to 0.1. Bacteria were diluted in Luria broth amended with MgSO₄ (2 mM) and CaCl₂ (10 mM) to a starting concentration of 10⁵ CFU ml⁻¹. If required, the medium was amended with 50 µg ml⁻¹ kanamycin and/or 100 µg ml⁻¹ ampicillin. Cultures were shaken at 150 rpm (double

orbital) at 28°C for 24 h in a plate reader. Optical density was measured every 30 min.

SDS-PAGE and Western blot

Western blots using polyclonal Anti-BcsC antibodies (GenScript) were carried out to establish whether BcsC was produced in the different generated mutants. Mutants were grown overnight and supplemented with antibiotics if required. The cells were transferred into 50 ml of the corresponding prewarmed medium and incubated at 28°C with vigorous shaking until an OD_{600nm} of 0.5 was reached. Cells carrying a pBAD18 based construct were induced with 0.2% (wt./vol.) arabinose and incubated overnight at 17°C with vigorous shaking. Cells were harvested (4000g, 20 min), lysed using Bacterial Protein Extraction Reagent B-PER (Thermo Fisher) (4 ml g⁻¹ pellet), lysozyme (8 µl g⁻¹ pellet) and DNase I (8 µl g⁻¹ pellet) and incubated for 15 min at RT in an overhead rotator. Two milliliters of each lysate was centrifuged at 10 000g for 20 min at 4°C. The supernatant was collected and stored at -20°C and the pellet was re-suspended in 100 µl 1× SDS-PAGE sample buffer [90 mM Tris-base, 2% (wt./vol.) SDS, 0.02% (wt./vol.) Bromophenol Blue, 20% (vol./vol.) glycerol in ultrapure H₂O (Satorius) and pH adjusted to 6.8]. Five microliters of each pellet sample was supplemented with 4 µl 1× SDS-PAGE sample buffer and 1 µl DTT (1 M) and boiled for 5 min at 95°C. Three microliters per sample were loaded on a 1 mm 7.5% resolving, 4% stacking gel and let run for 25 min at 200 V. The transfer was carried out using a TransBlot-Turbo System (BioRad) and a PVDF Transfer Pack and let run for 10 min (1.3 A, 25 V). The membrane was blocked [5% (wt./vol.) milk powder, 0.1% (wt./vol.) Triton X-100 in 1× PBS] for 1 h at RT. The membrane was washed three times with PBS before the rabbit anti-BcsC Antibody (GenScript) was added (1:1000 in blocking buffer) and incubated at RT for 1 h under constant shaking. The membrane was washed three times with PBS before the secondary goat anti-rabbit IgG (HRP) antibody (abcam) was added (1/2500× in blocking buffer) and incubated for 1 h at RT with constant shaking. Signals were detected through chemiluminescence by applying 10 ml ECL buffer (100 mM Tris, pH 8.6), 22 µl p-coumaric acid, 50 µl luminol and 3 µl H₂O directly onto the membrane for 90 s (Mruk and Cheng, 2011). The chemiluminescence solution was carefully removed and signals were detected by an Azure Biosystem C300 (Azur Biosystems, Dublin, CA, USA).

Visualization of cellulose production

To investigate alterations in the cellulose production provoked by the gene modifications, qualitative cellulose

visualization was performed. Luria agar was amended with 40 $\mu\text{g ml}^{-1}$ Congo Red and 20 $\mu\text{g ml}^{-1}$ Coomassie Brilliant Blue. 100 $\mu\text{g ml}^{-1}$ Ampicillin, 0.2% (wt./vol.) glucose or 0.2% (wt./vol.) arabinose were added if required. Bacteria were spotted (5 μl per sample) on plates and incubated for 2 days at RT. Bacteria with the ability to produce cellulose appeared as pink colonies while non-producing bacteria remained white (Colvin and Witter, 1983; Castiblanco and Sundin, 2016).

In vitro infection assays

Overnight cultures of *E. amylovora* CFBP 1430 were washed twice in sterile SM buffer and $\text{OD}_{600\text{nm}}$ was adjusted to reach approximately 10^7 CFU ml^{-1} . Subsequently, 20 μl of the washed cells were transferred to 1960 μl Luria broth (10 g L^{-1} tryptone, 10 g L^{-1} NaCl, 5 g L^{-1} yeast extract, 2 mM MgSO_4 , 10 mM CaCl_2) and amended with either 20 μl sterile SM buffer or with 20 μl bacteriophage (10^{10} PFU ml^{-1}). The mixtures were then added to 96 well flat-bottom plates and incubated at 25°C with double orbital shaking for 30 h in a plate reader. $\text{OD}_{600\text{nm}}$ measurements were carried out every half hour. For experiments involving the cellulose-binding dye Congo Red, different concentrations of Congo Red (10, 20, 40 $\mu\text{g ml}^{-1}$) and Coomassie Brilliant Blue (5, 10, 20 $\mu\text{g ml}^{-1}$) were added. To test the impact of cellulase and the purified protein Gp95_{S6} on bacterial growth and phage infectivity, the proteins were tested at different concentrations.

Detached flower assays

A detached flower assay using fresh Golden Delicious blossoms from 2-year-old apple trees was carried out to monitor virulence of *E. amylovora* mutants (Pusey, 1997). Blossoms were treated with either *E. amylovora* CFBP1430, *E. amylovora* CFBP1430 [pBAD18] or PBS as mock infection. Racks were cleaned and autoclaved before the experiment and 24 wells per rack were filled with 2 ml H_2O . The wells were sealed with scotch tape, which was perforated using a syringe. Blossom stems were freshly cut to ensure water uptake before being transferred through the scotch tape. Bacteria grown overnight on plates were scratched off and carefully re-suspended in PBS. $\text{OD}_{600\text{nm}}$ was adjusted to 1.0 and a 1:50 dilution was performed (approx. 10^7 CFU ml^{-1}). The blossoms were inoculated by pipetting 20 μl bacterial suspension or PBS directly onto the receptacle. S6 was added at a concentration of 10^8 PFU ml^{-1} by pipetting 5 μl phage suspension onto the receptacle. Each storage box (5 L) was laid out with paper towels and filled with three racks. To ensure humidity, 100 ml H_2O was added per box. The blossoms were stored at 26°C for 4–5 days.

The readout was performed according to an adjusted rating system (Llop *et al.*, 2017). Healthy blossoms without disease symptoms were classified as grade 1. Visible symptoms on the blossom (browning of the calix) were referred to as grade 2. Blossoms with infection spreading from the calix to the stipe of the blossoms corresponded to grade 3.

Protein expression and purification

For expression and purification, the genes gp94 and gp95 were cloned into pQE30 (QIAGEN). Primers to amplify the different genes were designed with BamHI or SacI and HindIII restriction sites (Supplementary Table 2). Amplified products with the correct length were recovered from a 1% (wt./vol.) agarose gel before a double digest using BamHI and HindIII (NEB, in Buffer 3.1 with a twofold excess of HindIII, 37°C for 1 h) was performed for gp95 and the vector pQE30. The digested fragments were purified using the DNA Clean and concentrator kit (Zymo) before ligation was carried out (T4 ligase, temperature gradient overnight). Ligated plasmids were introduced into *E. coli* XL1-Blue by electroporation (1.7 kV) and recovered in SOC medium for 1 h at 37°C before plating on Luria agar plates containing 100 $\mu\text{g ml}^{-1}$ ampicillin. Colonies were screened for correct plasmid integration by PCR and sequencing of the generated products. *Escherichia coli* XL1-Blue with the expression vectors were grown in Luria broth amended with 100 $\mu\text{g ml}^{-1}$ ampicillin until an $\text{OD}_{600\text{nm}}$ of 0.3 was reached. Protein expression was induced with 0.1 mM IPTG. Expression was carried out at 17°C overnight. Cells were harvested and lysed as mentioned above. The protein was purified by an immobilized metal affinity chromatography. The nickel-nitrilotriacetic acid agarose column was prepared according to the manufacturer's instruction (QIAGEN). The column was equilibrated with 5-column volumes of lysis buffer (pH 8.0, 50 mM NaH_2PO_4 , 300 mM NaCl, 10 mM Imidazole) supplemented with 500 μl BPER, before the lysate was loaded. The column was subsequently washed five times with a column volume of wash buffer (pH 8.0, 50 mM NaH_2PO_4 , 300 mM NaCl, 20 mM Imidazole). Elution buffer (pH 8.0, 50 mM NaH_2PO_4 , 300 mM NaCl, 250 mM Imidazole) was used to release bound proteins. Fractions with the highest protein content were re-purified. Purified proteins were dialyzed against dialysis buffer [pH 8.0, 50 mM NaH_2PO_4 , 100 mM NaCl, 0.005% (vol./vol.) Tween 20] at 4°C for 24 h.

Cellulase activity

A modified protocol of Ghose, 1987 was used (Ghose, 1987) to measure the amount of released

glucose after incubation with putative cellulases. The substrate carboxymethyl cellulose sodium salt (CMC) or H₂O as control as well as the phages S6, L1 and Y2 (all 5×10^9 PFU ml⁻¹ and 5×10^8 PFU ml⁻¹) or the phage proteins (0.1–0.001 mg ml⁻¹) and the cellulase from *Trichoderma reesei* (aqueous solution, >700 units g⁻¹ Sigma Aldrich, Switzerland) as positive control, were prewarmed to 40°C. A total of 250 µl substrate was combined with 250 µl phage, phage proteins or cellulase in a 2 ml test tube and mixed well. The tubes were subsequently incubated at 40°C for exactly 10 min. Afterwards, 1 ml of Dinitrosalicylic acid solution (32.85 mM DNS, 0.3 M NaOH, 1.05 M potassium sodium tartrate, 87.5 mM lactose in H₂O) was added to each tube and the reaction was stopped by boiling the samples at 100°C for 15 min. The samples were centrifuged at 3000g for 4 min. Finally, OD_{540nm} was measured. A standard curve with known quantities of glucose (5, 10, 15 µmol L⁻¹) and water was performed according to the protocol described above.

Acknowledgements

This work was funded by the Swiss National Science Foundation (SNF) grant 310030_156947. L.E.K., Y.B., M.J.L. and L.F. designed the experiments. L.E.K., N.H., Y.B. and K.F. performed the experiments. L.E.K., Y.B., C.P., and L.F. carried out analysis of the data. The manuscript was written by L.E.K., N.H., Y.B., C.P., M.J.L. and L.F.

References

- Adams, M.H. (1959) *Bacteriophages*: New York, NY: Interscience Publishers.
- Ahmad, I., Rouf, S.F., Sun, L., Cimmins, A., Shafeeq, S., Le Guyon, S., et al. (2016) BcsZ inhibits biofilm phenotypes and promotes virulence by blocking cellulose production in *Salmonella enterica* serovar Typhimurium. *Microb Cell Fact* **15**: 177. <https://doi.org/10.1186/s12934-016-0576-6>.
- Al-Ishaq, R.K., Skariah, S., and Büsselberg, D. (2020) Bacteriophage treatment: critical evaluation of its application on World Health Organization priority pathogens. *Viruses* **13**: 51. <https://doi.org/10.3390/v13010051>.
- Alonso-García, N., Inglés-Prieto, A., Sonnenberg, A., and De Pereda, J.M. (2009) Structure of the Calx-B domain of the integrin B4 subunit: insights into function and cation-independent stability. *Acta Crystallogr D Biol Crystallogr* **65**: 858–871. <https://doi.org/10.1107/S0907444909018745>.
- An, X., Zong, Z., Zhang, Q., Li, Z., Zhong, M., Long, H., et al. (2022) Novel thermo-alkali-stable cellulase-producing *Serratia* sp. AXJ-M cooperates with *Arthrobacter* sp. AXJ-M1 to improve degradation of cellulose in papermaking black liquor. *J Hazard Mater* **421**: 126811. <https://doi.org/10.1016/j.jhazmat.2021.126811>.
- Aspeborg, H., Coutinho, P.M., Wang, Y., Brumer, H., and Henrissat, B. (2012) Evolution, substrate specificity and subfamily classification of glycoside hydrolase family 5 (GH5). *BMC Evol Biol* **12**: 186. <https://doi.org/10.1186/1471-2148-12-186>.
- Ayers, A.R., Ayers, S.B., and Goodman, R.N. (1979) Extracellular polysaccharide of *Erwinia amylovora*: a correlation with virulence. *Appl Environ Microbiol* **38**: 659–666.
- Bai, A.J., and Rai, V.R. (2011) Bacterial quorum sensing and food industry. *Compr Rev Food Sci Food Saf* **10**: 183–193. <https://doi.org/10.1111/j.1541-4337.2011.00150.x>.
- Bellemann, P., Bereswill, S., Berger, S., and Geider, K. (1994) Visualization of capsule formation by *Erwinia amylovora* and assays to determine amylovoran synthesis. *Int J Biol Macromol* **16**: 290–296.
- Bereswill, S., and Geider, K. (1997) Characterization of the rcsB gene from *Erwinia amylovora* and its influence on exopolysaccharide synthesis and virulence of the fire blight pathogen. *J Bacteriol* **179**: 1354–1361. <https://doi.org/10.1128/jb.179.4.1354-1361.1997>.
- Berghem, L.E., and Petersson, L.G. (1973) The mechanism of enzymatic cellulose degradation. Purification of a cellulolytic enzyme from *Trichoderma viride* active on highly ordered cellulose. *Eur J Biochem* **37**: 21–30. <https://doi.org/10.1111/j.1432-1033.1973.tb02952.x>.
- Bertozzi Silva, J., Storms, Z., Sauvageau, D., and Silva, J. (2016) Host receptors for bacteriophage adsorption. *FEMS Microbiol Lett* **363**: fnw002. <https://doi.org/10.1093/femsle/fnw002>.
- Bonn, W.G., and van der Zwet, T. (2000) Distribution and economic importance of fire blight. In *Fire Blight: The Disease and Its Causative Agent, Erwinia Amylovora*, Vanneste, J.L. (ed): Wallingford, UK: CAB International, pp. 37–53.
- Born, Y., Fieseler, L., Klumpp, J., Eugster, M.R., Zurfluh, K., Duffy, B., and Loessner, M.J. (2014) The tail-associated depolymerase of *Erwinia amylovora* phage L1 mediates host cell adsorption and enzymatic capsule removal, which can enhance infection by other phage. *Environ Microbiol* **16**: 2168–2180. <https://doi.org/10.1111/1462-2920.12212>.
- Born, Y., Fieseler, L., Marazzi, J., Lurz, R., Duffy, B., and Loessner, M.J. (2011) Novel virulent and broad-host-range *Erwinia amylovora* bacteriophages reveal a high degree of mosaicism and a relationship to *Enterobacteriaceae* phages. *Appl Environ Microbiol* **77**: 5945–5954. <https://doi.org/10.1128/AEM.03022-10>.
- Born, Y., Fieseler, L., Thöny, V., Leimer, N., Duffy, B., and Loessner, M.J. (2017) Engineering of bacteriophages Y2::dpoL1-C and Y2::luxAB for efficient control and rapid detection of the fire blight pathogen, *Erwinia amylovora*. *Appl Environ Microbiol* **83**: e00341–e00317. <https://doi.org/10.1128/AEM.00341-17>.
- Broeker, N.K., and Barbirtz, S. (2017) Not a barrier but a key: how bacteriophages exploit host's O-antigen as an essential receptor to initiate infection. *Mol Microbiol* **105**: 353–357. <https://doi.org/10.1111/mmi.13729>.
- Brüssow, H., and Hendrix, R.W. (2002) Phage genomics: small is beautiful. *Cell* **108**: 13–16.
- Carder, J.H. (1986) Detection and quantitation of cellulase by Congo red staining of substrates in a cup-plate diffusion assay. *Anal Biochem* **153**: 75–79. [https://doi.org/10.1016/0003-2697\(86\)90063-1](https://doi.org/10.1016/0003-2697(86)90063-1).
- Casjens, S.R. (2005) Comparative genomics and evolution of the tailed-bacteriophages. *Curr Opin Microbiol* **8**: 451–458. <https://doi.org/10.1016/j.mib.2005.06.014>.

- Castiblanco, L.F., and Sundin, G.W. (2016) Cellulose production, activated by cyclic di-GMP through BcsA and BcsZ, is a virulence factor and an essential determinant of the three-dimensional architectures of biofilms formed by *Erwinia amylovora* Ea1189. *Mol Plant Pathol* **19**: 90–103. <https://doi.org/10.1111/mpp.12501>.
- Cobián Güemes, A.G., Youle, M., Cantú, V.A., Felts, B., Nulton, J., and Rohwer, F. (2016) Viruses as winners in the game of life. *Annu Rev Virol* **3**: 197–214. <https://doi.org/10.1146/annurev-virology-100114-054952>.
- Colvin, J.R., and Witter, D.E. (1983) Congo red and calcofluor white inhibition of *Acetobacter xylinum* cell growth and of bacterial cellulose microfibril formation: isolation and properties of a transient, extracellular glucan related to cellulose. *Protoplasma* **116**: 34–40. <https://doi.org/10.1007/BF01294228>.
- Das, S., Noe, J.C., Paik, S., and Kitten, T. (2005) An improved arbitrary primed PCR method for rapid characterization of transposon insertion sites. *J Microbiol Methods* **63**: 89–94. <https://doi.org/10.1016/J.MIMET.2005.02.011>.
- Datta, P.K., Hanson, K.R., and Whitaker, D.R. (1963) Improved procedures for preparation and characterization of Myrothecium cellulase. 3. Molecular weight, amino acid composition, terminal residues, and other properties. *Can J Biochem Physiol* **41**: 697–705.
- Edmunds, A.C., Castiblanco, L.F., Sundin, G.W., and Waters, C.M. (2013) Cyclic di-GMP modulates the disease progression of *Erwinia amylovora*. *J Bacteriol* **195**: 2155–2165. <https://doi.org/10.1128/JB.02068-12>.
- Eriksson, K.-E., and Pettersson, B. (1975) Extracellular enzyme system utilized by the fungus *Sporotrichum pulverulentum* (*Chrysosporium lignorum*) for the breakdown of cellulose: 3. Purification and physico-chemical characterization of an exo-1,4- β -glucanase. *Eur J Biochem* **51**: 213–218. <https://doi.org/10.1111/j.1432-1033.1975.tb03921.x>.
- Fehmel, F., Feige, U., Niemann, H., and Stirn, S. (1975) *Escherichia coli* capsule bacteriophages. VII. Bacteriophage 29-host capsular polysaccharide interactions. *J Virol* **16**: 591–601.
- Fujiwara, A., Fujisawa, M., Hamasaki, R., Kawasaki, T., Fujie, M., and Yamada, T. (2011) Biocontrol of *Ralstonia solanacearum* by treatment with lytic bacteriophages. *Appl Environ Microbiol* **77**: 4155–4162. <https://doi.org/10.1128/AEM.02847-10>.
- Galán, J.E., Ginocchio, C., and Costeas, P. (1992) Molecular and functional characterization of the Salmonella invasion gene invA: homology of InvA to members of a new protein family. *J Bacteriol* **174**: 4338–4349.
- Geider, K. (2000) Exopolysaccharides of *Erwinia amylovora*: structure, biosynthesis, regulation, role in pathogenicity of amylovoran and levan. In *Fire Blight: The Disease and Its Causative Agent, Erwinia Amylovora*, Vanneste, J.L. (ed). Wallingford: CAB International, pp. 117–140.
- Ghose, T.K. (1987) Measurement of cellulase activities. *Pure Appl Chem* **59**: 257–268.
- Gibson, D.G., Young, L., Chuang, R.-Y.Y., Venter, J.C., Hutchison III, C.A., Smith, H.O., et al. (2009) Enzymatic assembly of DNA molecules up to several hundred kilobases. *Nat Methods* **6**: 343–345. <https://doi.org/10.1038/NMETH.1318>.
- Gill, J.J., Svircev, A.M., Smith, R., and Castle, A.J. (2003) Bacteriophages of *Erwinia amylovora*. *Appl Environ Microbiol* **69**: 2133–2138. <https://doi.org/10.1128/aem.69.4.2133-2138.2003>.
- Guerrero-Ferreira, R.C., Viollier, P.H., Ely, B., Poindexter, J. S., Georgieva, M., Jensen, G.J., and Wright, E.R. (2011) Alternative mechanism for bacteriophage adsorption to the motile bacterium *Caulobacter crescentus*. *Proc Natl Acad Sci U S A* **108**: 9963–9968. <https://doi.org/10.1073/pnas.1012388108>.
- Guzman, L.L.M., Belin, D., Carson, M.J., and Beckwith, J. (1995) Tight regulation, modulation, and high-level expression by vectors containing the arabinose pBAD promoter. *J Bacteriol* **177**: 4121–4130.
- Halliwell, G., Griffin, M., and Vincent, R. (1972) The role of component C 1 in cellulolytic systems. *Biochem J* **127**: 43P. <https://doi.org/10.1042/bj1270043pa>.
- Hanahan, D. (1983) Studies on transformation of *Escherichia coli* with plasmids. *J Mol Biol* **166**: 557–580. [https://doi.org/10.1016/S0022-2836\(83\)80284-8](https://doi.org/10.1016/S0022-2836(83)80284-8).
- Hatfull, G.F. (2008) Bacteriophage genomics. *Curr Opin Microbiol* **11**: 447–453. <https://doi.org/10.1016/j.mib.2008.09.004>.
- Hsieh, P.F., Lin, H.H., Lin, T.L., Chen, Y.Y., and Wang, J.T. (2017) Two T7-like bacteriophages, K5-2 and K5-4, each encodes two capsule depolymerases: isolation and functional characterization. *Sci Rep* **7**: 4624. <https://doi.org/10.1038/s41598-017-04644-2>.
- Hsu, C.R., Lin, T.L., Pan, Y.J., Hsieh, P.F., and Wang, J.T. (2013) Isolation of a bacteriophage specific for a new capsular type of *Klebsiella pneumoniae* and characterization of its polysaccharide depolymerase. *PLoS One* **8**: e70092. <https://doi.org/10.1371/journal.pone.0070092>.
- Kazmierczak, K.M., and Rothman-Denes, L.B. (2006) Bacteriophage N4. In *The Bacteriophages*, Vol. **2nd**, Calendar, R. (ed): New York, NY: Oxford University Press, pp. 302–314.
- Kharadi, R.R., Castiblanco, L.F., Waters, C.M., and Sundin, G.W. (2019) Phosphodiesterase genes regulate amylovoran production, biofilm formation, and virulence in *Erwinia amylovora*. *Appl Environ Microbiol* **85**: e02233-18. <https://doi.org/10.1128/AEM.02233-18>.
- Knecht, L.E., Veljkovic, M., and Fieseler, L. (2020) Diversity and function of phage encoded depolymerases. *Front Microbiol* **10**: 2949. <https://doi.org/10.3389/fmicb.2019.02949>.
- Koczan, J.M., Lenneman, B.R., McGrath, M.J., and Sundin, G.W. (2011) Cell surface attachment structures contribute to biofilm formation and xylem colonization by *Erwinia amylovora*. *Appl Environ Microbiol* **77**: 7031–7039. <https://doi.org/10.1128/AEM.05138-11>.
- Koczan, J.M., McGrath, M.J., Zhao, Y., and Sundin, G.W. (2009) Contribution of *Erwinia amylovora* exopolysaccharides amylovoran and levan to biofilm formation: implications in pathogenicity. *Phytopathology* **99**: 1237–1244. <https://doi.org/10.1094/PHYTO-99-11-1237>.
- Koo, H.M., Song, S.H., Pyun, Y.R., and Kim, Y.S. (1998) Evidence that a b-1,4-endoglucanase secreted by *Acetobacter xylinum* plays an essential role for the formation of cellulose fiber. *Biosci Biotechnol Biochem* **62**: 2257–2259.

- Labrie, S.J., Samson, J.E., and Moineau, S. (2010) Bacteriophage resistance mechanisms. *Nat Rev Microbiol* **8**: 317–327. <https://doi.org/10.1038/nrmicro2315>.
- Lamas, A., Miranda, J.M., Vázquez, B., Cepeda, A., and Franco, C.M. (2016) Biofilm formation, phenotypic production of cellulose and gene expression in *Salmonella enterica* decrease under anaerobic conditions. *Int J Food Microbiol* **238**: 63–67.
- Latka, A., Leiman, P.G., Drulis-Kawa, Z., and Briers, Y. (2019) Modeling the architecture of depolymerase-containing receptor binding proteins in *Klebsiella* phages. *Front Microbiol* **10**: 2649. <https://doi.org/10.3389/fmicb.2019.02649>.
- Latka, A., Maciejewska, B., Majkowska-Skrobek, G., Briers, Y., and Drulis-Kawa, Z. (2017) Bacteriophage-encoded virion-associated enzymes to overcome the carbohydrate barriers during the infection process. *Appl Microbiol Biotechnol* **101**: 3103–3119. <https://doi.org/10.1007/s00253-017-8224-6>.
- Le Quééré, B., and Ghigo, J.-M. (2009) BcsQ is an essential component of the *Escherichia coli* cellulose biosynthesis apparatus that localizes at the bacterial cell pole. *Mol Microbiol* **72**: 724–740. <https://doi.org/10.1111/j.1365-2958.2009.06678.x>.
- Lin, T.L., Hsieh, P.F., Huang, Y.T., Lee, W.C., Tsai, Y.T., Su, P.A., et al. (2014) Isolation of a bacteriophage and its depolymerase specific for K1 capsule of *Klebsiella pneumoniae*: implication in typing and treatment. *J Infect Dis* **210**: 1734–1744. <https://doi.org/10.1093/infdis/jiu332>.
- Lindberg, A.A. (1973) Bacteriophage receptors. *Annu Rev Microbiol* **27**: 205–241. <https://doi.org/10.1146/annurev.mi.27.100173.001225>.
- Llop, P., Cabrefiga, J., Smits, T.H.M., Dreö, T., Barbé, S., Pulawska, J., et al. (2017) *Erwinia amylovora* novel plasmid pEI70: complete sequence, biogeography, and role in aggressiveness in the fire blight phytopathogen. *PLoS One* **6**: e28651.
- Maes, M., Orye, K., Bobev, S., Devreese, B., Van Beeumen, J., De Bruyn, A., et al. (2001) Influence of amylovoran production on virulence of *Erwinia amylovora* and a different amylovoran structure in *E. amylovora* isolates from *Rubus*. *Eur J Plant Pathol* **107**: 839–844.
- Mansfield, J., Genin, S., Magori, S., Citovsky, V., Sriariyanum, M., Ronald, P., et al. (2012) Top 10 plant pathogenic bacteria in molecular plant pathology. *Mol Plant Pathol* **13**: 614–629. <https://doi.org/10.1111/j.1364-3703.2012.00804.x>.
- Marti, R., Zurfluh, K., Hagens, S., Pianezzi, J., Klumpp, J., and Loessner, M.J. (2013) Long tail fibres of the novel broad-host-range T-even bacteriophage S16 specifically recognize *Salmonella* OmpC. *Mol Microbiol* **87**: 818–834. <https://doi.org/10.1111/mmi.12134>.
- Mazur, O., and Zimmer, J. (2011) Apo- and cellopentaose-bound structures of the bacterial cellulose synthase subunit BcsZ. *J Biol Chem* **286**: 17601–17606. <https://doi.org/10.1074/jbc.M111.227660>.
- Momol, M.T., and Aldwinckle, H.S. (2000) Genetic diversity and host range of *Erwinia amylovora*. In *Fire Blight: The Disease and Its Causative Agent, Erwinia amylovora*, Vanneste, J.L. (ed). Wallingford: CAB International, pp. 55–72.
- Morgan, J.L.W., Strumillo, J., and Zimmer, J. (2013) Crystallographic snapshot of cellulose synthesis and membrane translocation. *Nature* **493**: 181–186. <https://doi.org/10.1038/nature11744>.
- Mruk, D.D., and Cheng, C.Y. (2011) Enhanced chemiluminescence (ECL) for routine immunoblotting. *Spermatogenesis* **1**: 121–122. <https://doi.org/10.4161/spmg.1.2.16606>.
- Myers, F.L., and Northcote, D.H. (1959) Partial purification and some properties of a cellulase from *Helix pomatia*. *Biochem J* **71**: 749–756. <https://doi.org/10.1042/bj0710749>.
- Oliveira, H., Costa, A.R., Konstantinides, N., Ferreira, A., Akturk, E., Sillankorva, S., et al. (2017) Ability of phages to infect *Acinetobacter calcoaceticus*-*Acinetobacter baumannii* complex species through acquisition of different pectate lyase depolymerase domains. *Environ Microbiol* **19**: 5060–5077. <https://doi.org/10.1111/1462-2920.13970>.
- Oliveira, H., Mendes, A., Fraga, A.G., Ferreira, A., Pimenta, A.I., Mil-Homens, D., et al. (2019) K2 capsule depolymerase is highly stable, is refractory to resistance, and protects larvae and mice from *Acinetobacter baumannii* sepsis. *Appl Environ Microbiol* **85**: e00934-19. <https://doi.org/10.1128/AEM.00934-19>.
- Omadjela, O., Narahari, A., Strumillo, J., Mérida, H., Mazur, O., Bulone, V., and Zimmer, J. (2013) BcsA and BcsB form the catalytically active core of bacterial cellulose synthase sufficient for *in vitro* cellulose synthesis. *Proc Natl Acad Sci U S A* **110**: 17856–17861. <https://doi.org/10.1073/pnas.1314063110>.
- Pan, Y.-J., Lin, T.-L., Chen, C.-C., Tsai, Y.-T., Cheng, Y.-H., Chen, Y.-Y., et al. (2017) *Klebsiella* phage Φ K64-1 encodes multiple depolymerases for multiple host capsular types. *J Virol* **91**: e02457-16. <https://doi.org/10.1128/jvi.02457-16>.
- Pires, D.P., Oliveira, H., Melo, L.D.R.R., Sillankorva, S., and Azeredo, J. (2016) Bacteriophage-encoded depolymerases: their diversity and biotechnological applications. *Appl Microbiol Biotechnol* **100**: 2141–2151. <https://doi.org/10.1007/s00253-015-7247-0>.
- Prokhorov, N.S., Riccio, C., Zdorovenko, E.L., Shneider, M. M., Browning, C., Knirel, Y.A., et al. (2017) Function of bacteriophage G7C esterase tailspike in host cell adsorption. *Mol Microbiol* **105**: 385–398. <https://doi.org/10.1111/mmi.13710>.
- Pusey, P.L. (1997) Crab apple blossoms as a model for research on biological control of fire blight. *Phytopathology* **87**: 1096–1102.
- Rakhuba, D.V., Kolomiets, E.I., Dey, E.S., Novik, G.I., Szwajcer Dey, E., and Novik, G.I. (2010) Bacteriophage receptors, mechanisms of phage adsorption and penetration into host cell. *Pol J Microbiol* **59**: 145–155. <https://doi.org/10.1016/j.micres.2015.01.008.1.94>.
- Roach, D.R., Sjaarda, D.R., Castle, A.J., and Svircev, A.M. (2013) Host exopolysaccharide quantity and composition impact *Erwinia amylovora* bacteriophage pathogenesis. *Appl Environ Microbiol* **79**: 3249–3256. <https://doi.org/10.1128/AEM.00067-13>.
- Römling, U., and Galperin, M.Y. (2015) Bacterial cellulose biosynthesis: diversity of operons, subunits, products, and functions. *Trends Microbiol* **23**: 545–557. <https://doi.org/10.1016/j.tim.2015.05.005>.

- Sambrook, J., and Russell, D.W. (2001) *Molecular Cloning*, Vol. 1: New York, NY: Cold Spring Harbor Laboratory Press.
- Shin, H., Lee, J.-H.H., Kim, H., Choi, Y., Heu, S., and Ryu, S. (2012) Receptor diversity and host interaction of bacteriophages infecting *Salmonella enterica* serovar Typhimurium. *PLoS One* **7**: e43392. <https://doi.org/10.1371/journal.pone.0043392>.
- Skorupski, K., and Taylor, R.K. (1996) Positive selection vectors for allelic exchange. *Gene* **169**: 47–52.
- The UniProt Consortium. (2019) UniProt: a worldwide hub of protein knowledge. *Nucleic Acids Res* **47**: D506–D515. <https://doi.org/10.1093/nar/gky1049>.
- Thomson, S.V. (2000) Epidemiology of fire blight. In *Fire Blight: The Disease and Its Causative Agent, Erwinia Amylovora*, Vanneste, J.L. (ed): Wallingford, UK: CAB International, pp. 9–36.
- Tuleski, T.R., de Baura, V.A., Donatti, L., de Oliveira Pedrosa, F., Maltempi de Souza, E., and Monteiro, R.A. (2019) Cellulose production increases sorghum colonization and the pathogenic potential of *Herbaspirillum rubrisubalbicans* M1. *Sci Rep* **9**: 4041. <https://doi.org/10.1038/s41598-019-40600-y>.
- Vanneste, J.L. (2000) What is fire blight? Who is *Erwinia amylovora*? How to control it? In *Fire Blight*. Wallingford: CAB International, pp. 1–6.
- Vanneste, J.L., and Eden-Green, S. (2000) Migration of *Erwinia amylovora* in host plant tissues. In *Fire Blight: The Disease and its Causative Agent, Erwinia amylovora*, Vanneste, J.L. (ed). Wallingford: CAB International, pp. 73–83.
- Waterhouse, A., Bertoni, M., Bienert, S., Studer, G., Tauriello, G., Gumienny, R., et al. (2018) SWISS-MODEL: homology modelling of protein structures and complexes. *Nucleic Acids Res* **46**: W296–W303. <https://doi.org/10.1093/nar/gky427>.
- Wei, Z., Kim, J.F., and Beer, S.V. (2000) Regulation of *hrp* genes and type III protein secretion in *Erwinia amylovora* by HrpX/HrpY, a novel two-component system, and HrpS. *Mol Plant Microbe Interact* **13**: 1251–1262. <https://doi.org/10.1094/MPMI.2000.13.11.1251>.
- Whitney, J.C., Hay, I.D., Li, C., Eckford, P.D.W., Robinson, H., Amaya, M.F., et al. (2011) Structural basis for alginate secretion across the bacterial outer membrane. *Proc Natl Acad Sci U S A* **108**: 13083–13088. <https://doi.org/10.1073/pnas.1104984108>.
- Zimmermann, L., Stephens, A., Nam, S.Z., Rau, D., Kübler, J., Lozajic, M., et al. (2018) A completely reimplemented MPI bioinformatics toolkit with a new HHpred server at its core. *J Mol Biol* **430**: 2237–2243. <https://doi.org/10.1016/j.jmb.2017.12.007>.

Supporting Information

Additional Supporting Information may be found in the online version of this article at the publisher's web-site:

Fig. 1. Latency period and burst size of S6 were determined by one step growth curve. S6 is revealed to have a latency period of 110 min with a burst size of ≥ 59 progeny phages.

Table 1. Bacterial strains, plasmids, phages, and antibodies used in this study.

Table 2. Oligonucleotides used in this study.